BIOCHEMISTRY
including biophysical chemistry & molecular biology

Article

pubs.acs.org/biochemistry

Nuclear Magnetic Resonance Analysis of the Acetylation Pattern of the Neuronal Tau Protein

Amina Kamah,[†] Isabelle Huvent,[†] François-Xavier Cantrelle,[†] Haoling Qi,[†,‡] Guy Lippens,[†] Isabelle Landrieu,[†,‡] and Caroline Smet-Nocca*[,†]

[†]Université de Lille-Nord de France, CNRS UMR 8576, Institut Fédératif de Recherches 147, Villeneuve d'Ascq, France

[‡]Interdisciplinary Research Institute, Campus CNRS-Parc de la haute-borne, 50 avenue de Halley, 59658 Villeneuve d'Ascq Cedex, France

Supporting Information

ABSTRACT: Lysine acetylation of the neuronal Tau protein was described as a novel mechanism of posttranslational regulation of Tau functions with important outcomes in microtubule binding and aggregation processes related to Alzheimer's disease. Here, we unravel at a per-residue resolution the acetylation pattern of full-length Tau by the Creb-binding protein (CBP) acetyltransferase using high-resolution nuclear magnetic resonance spectroscopy. Our study gives a quantitative overview of CBP-mediated acetylation and examines the catalytic proficiency because the nonenzymatic reaction with acetyl-coenzyme A occurs *in vitro*. Furthermore, we have investigated with this characterized acetylated Tau the effect of acetylation on Tau fibrillization in a heparin-induced aggregation assay and on heparin binding.

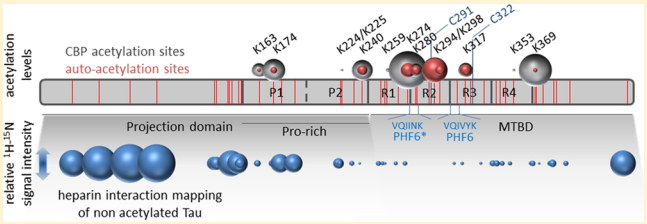

Protein acetylation, discovered many years ago, has recently gained prominence as a ubiquitous posttranslational modification (PTM). Like phosphorylation, it was found to affect the localization, degradation, interactions, and activity of many proteins involved in diverse cellular functions such as transcription, cytoskeleton dynamics, metabolism, autophagy, cellular signaling, and kinase regulation.[1] Cross-talk with another PTM, the covalent addition of ubiquitin that often marks a protein for proteosomal degradation, is one possible molecular mechanism through which acetylation can exert its function.[2] Recently, lysine acetylation was shown to play an important role in Tau pathology associated with the neurodegenerative processes of Alzheimer's disease (AD). Reduced clearance of (hyper)phosphorylated Tau leading to its accumulation under the form of intraneuronal tangles is one of the characteristic hallmarks of AD. The detection of soluble Tau forms ubiquitinated at several positions in AD brain tissue,[3] of phosphorylated and ubiquitinated Tau oligomers at the postsynaptic densities,[4] and of ubiquitin in the paired helical filaments (PHFs) that make up those tangles[5] points to a defective clearance mechanism at different stages of the disease.

To investigate whether Tau acetylation contributes to a defect in ubiquitin-proteasome degradation of Tau, Min et al. first studied the *in vitro* acetylation of Tau by the recombinant p300 acetyltransferase.[6] As many as 23 lysine residues over a total of 44 were found to be acetylated, most of them being located in the microtubule-binding domain. Mass spectrometry identified a Tau peptide with three acetylated lysines at positions K163, K174, and K180, and this peptide allowed the generation of a first acetyl-Tau specific antibody. With this antibody, the authors determined that p300 is the prominent enzyme that generates the Tau acetylation pattern at this particular epitope in primary neurons, and that the histone deacetylase SIRT1 removes the acetyl groups from these lysines. SIRT1 was equally found to be important *in vivo* in the maintenance of the acetylation pattern at another motif of endogenous Tau, comprising the K274 and K281 sites. Interestingly, a cross-talk between acetylation and phosphorylation has been implicated in the accumulation of abnormally phosphorylated Tau that is known to promote dissociation from microtubules and Tau fibrillization. Phosphorylated Tau is physiologically degraded via the proteasome-mediated pathway,[7,8] and its accumulation could be due to a clearance failure potentially associated with acetylation events. Acetylation increases the lifetime of Tau and particularly of phosphorylated Tau forms, in agreement with the previous finding that reduced SIRT1 levels correlate with the accumulation and aggregation of Tau in AD brains.[6,9] Interference with the ubiquitin-proteasomal degradation of phospho-Tau hence is a first role for acetylation in AD, and the combined results suggest that lysine modification would precede Tau hyperphosphorylation in the disease process.

A more direct effect of lysine acetylation on the physiological and pathological aspects of Tau was determined in a second study.[10] At the molecular level, lysine residues such as K274 and K281 have been shown to provide a molecular interface

Received: January 3, 2014
Revised: April 4, 2014
Published: April 7, 2014

   dx.doi.org/10.1021/bi500006v | *Biochemistry* 2014, 53, 3020−3032

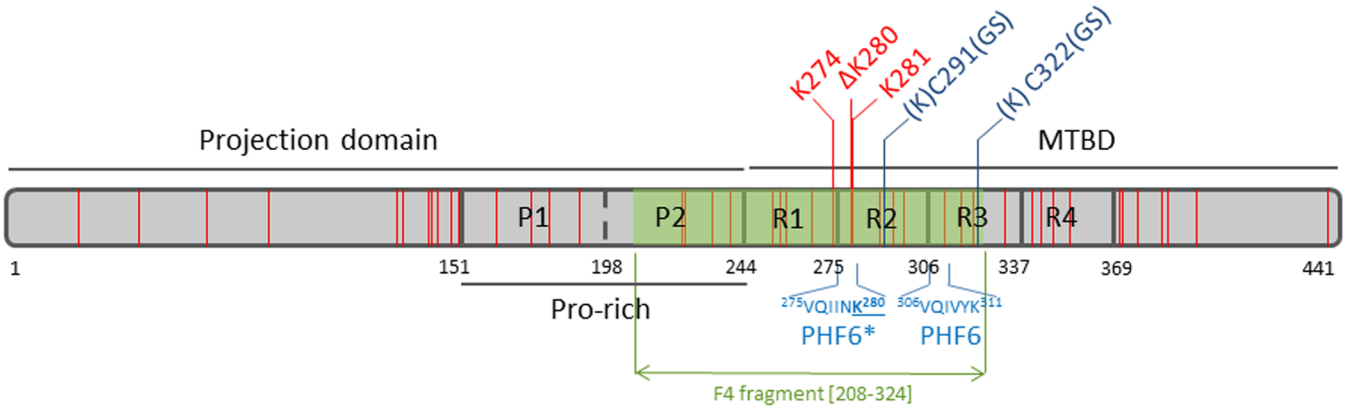

Figure 1. Schematic representation of the domains of the longest Tau isoforms (441 residues) and the position of the 44 lysine residues along the sequence. The Tau-F4 fragment encompassing residues 208−324 is colored green. Lysine residues colored red have been described either as hot spots for microtubule binding (K274 and K281)[11] or as a site of mutation in FTDP (K280) that affects both microtubule stabilization and aggregation kinetics.[14,49] Both KCGS motifs are colored blue. The PHF6* and PHF6 peptides at the beginning of repeats R2 and R3, respectively, implicated in nucleation and PHF assembly are colored blue. MTBD represents the microtubule-binding repeat domain and Pro-rich the proline-rich domain.

with microtubules[11] while deletion of K280 (ΔK280) was identified as an etiological factor in the familial form of the FTDP-17 tauopathy contributing to impaired microtubule assembly and enhancement of aggregation into PHFs *in vitro*.[12−14] These suggest that lysine acetylation has the potency to modulate Tau physiopathological functions. *In vitro* tubulin polymerization by the K18 fragment was indeed impaired when the Tau fragment was initially acetylated by the CBP enzyme, a close homologue of the previously cited p300 acetyltransferase, and the same reduced level of tubulin bundling was observed at the cellular level upon acetylation of full-length Tau. Despite the nearly identical experimental setup for the *in vitro* acetylation assay and subsequent mass spectrometry-based determination of the resulting PTM pattern, the single site in common with those investigated in the previous study was K163, outside of the MTBR. Other sites that were found to be modified at a substantial level were K280, K281, and K369, all three in the MTBR. Beyond impairing microtubule assembly, acetylation further stimulated the heparin-induced formation of amyloid fibers of K18 and full-length Tau, thereby mimicking the *in vitro* effect of the ΔK280 deletion of Tau. This, together with the important effect of the sole K280 acetylation on MT assembly, motivated the production of a monoclonal antibody against the Ac-K280 epitope. In brain tissues of patients with various tauopathies (but not Pick's disease, characterized by a dominant 3R isoform in which K280 is absent), this antibody allowed detection of acetylated Tau, and acetylation staining colocalized with the AT8 hyperphosphorylated amyloid forms of Tau in transgenic mouse models[15,16] or human tauopathies. The acetylated forms of Tau were found only in diseased tissues at all stages of AD and are here rather concomitant with pathological epitopes found at late stages of AD such as Alz50/MC-1, AT100, TG-3, or PHF-1.[17] Beyond interference with Tau degradation, acetylation at specific sites hence can lead to altered microtubule assembly and an increased level of PHF formation, providing a second, more active role for the PTM. Hence, acetylation could be used as a biomarker of AD, and enzymes involved in the dynamics of Tau acetylation could be targeted in innovative drug design strategies in AD and other tauopathies. Furthermore, Tau acetylation could be an important event in mediating Tau spreading because Tau acetylation is absent of intraneuronal inclusions of argyrophilic grain disease, which is an age-associated atypical 4R tauopathy where Tau pathology is not always correlated with clinical progression.[18]

Another deacetylase, HDAC6, was found to be expressed at high levels in AD brains.[19] As it directly removes acetyl groups from Tau,[10] this suggests an opposite role for acetylation in the disease. The effect was mapped to acetylation at the KXGS motifs and notably concerns K259 and K353 in the two-KIGS motif. Amazingly, the acetylation of these two lysines as detected by an Ac-KIGS antibody reduces the the level of formation of Tau fibers, as observed in an *in vitro* aggregation assay with dextran sulfate as the polyanionic inducer. K259 acetylation was furthermore found to be exclusive with the MARK2-catalyzed phosphorylation at S262, a PTM that has been shown to weaken the interaction with microtubules[20] and to inhibit Tau aggregation.[21]

In view of the conflicting results concerning the acetylation patterns generated by p300/CBP and their functional aspect, we decided to apply a completely independent method to assert in a quantitative manner the acetylation pattern of Tau. We previously showed on small peptides that nuclear magnetic resonance (NMR) spectroscopy can be used to map and quantify the modified lysines,[22] and a subsequent study extended this method to provide a kinetic view of acetylation of a histone H4 peptide.[23] We describe here for the first time the study of acetylation posttranslational modification in the context of an entire protein by NMR spectroscopy. Full-length Tau, with its 44 lysine residues, evidently is more challenging, motivating us to study also the acetylation pattern of a smaller but functional fragment, Tau-F4, that spans residues 208−324 (Figure 1). We simultaneously address the recently discovered autoacetylation of Tau, whereby the mere presence of acetyl-CoA was found to lead to acetyl integration.[24] Finally, with these well-characterized samples, we evaluate the influence of acetylation on the aggregation kinetics of Tau induced by heparin.

MATERIALS AND METHODS

Production of ^{15}N- and ^{13}C-Labeled or ^{15}N-Labeled Tau and Tau-F4 Fragments in *Escherichia coli*. The Tau441 (residues 1−441 of human MAPT) and Tau-F4 (residues 208−324) fragments in their wild-type or mutant

dx.doi.org/10.1021/bi500006v | *Biochemistry* 2014, 53, 3020−3032

forms (C291S, C322S, or C291S/C322S) were produced in the *E. coli* BL21(DE3) strain carrying the pET15b recombinant plasmid (Novagen). Cells were grown at 37 °C in M9 minimal medium containing 4 g/L glucose or 2 g/L [$^{13}C_6$]glucose for the expression of ^{13}C-labeled proteins, 1 g/L [^{15}N]ammonium chloride, 1 mM $MgSO_4$, MEM vitamin cocktail (Sigma), and ampicillin (100 mg/L). For selective [^{15}N]Lys and uniform ^{13}C labeling, bacteria were grown in M9 medium as described above with 2 g/L [$^{13}C_6$]glucose and 1 g/L [^{14}N]ammonium chloride while 100 mg of [^{15}Nα,ε/^{13}C]lysine was added 20 min before induction. The induction phase was initiated by addition of 0.5 mM isopropyl 1-thio-β-D-galactopyranoside (IPTG) and continued at 37 °C for 2 h. Cells were harvested by centrifugation, and the pellet was washed in phosphate-buffered saline. For full-length Tau (Tau441), the bacterial pellet was resuspended in 50 mM Na_iPO_4 (pH 6.3), 2 mM dithiothreitol, 2 mM EDTA, and 0.5% Triton X-100 complemented with a protease inhibitor cocktail (Complete, Roche). The soluble extract was obtained by incubation of the cell suspension at 4 °C for 30 min with 0.2 mg/mL lysozyme and DNase, followed by a brief sonication step, and centrifugation at 25000*g* for 30 min. The soluble extracts were incubated at 75 °C for 15 min, and the soluble proteins were isolated by centrifugation at 6000*g* for 30 min and purified by cation exchange chromatography (HiTrap SP, GE Healthcare). The Tau-F4 fragment carrying an N-terminal histidine tag was purified by being heated for 15 min at 75 °C, followed by affinity purification on Ni^{2+} resin (HiTrap Chelating, GE Healthcare). Homogeneous fractions as checked by denaturing polyacrylamide gel electrophoresis were pooled and buffer-exchanged in 50 mM ammonium bicarbonate prior to lyophilization. A second step of purification by reverse phase chromatography on a C18 column (Zorbax C18 300SB, Agilent Technologies) was performed.

Production of the Recombinant CBP[1202−1848] Fragment with Acetyltransferase Activity. A CBP fragment corresponding to residues 1202−1848 (mouse CBP) was overexpressed in the BL21(DE3) strain as a GST fusion protein (pGEX-6P-1 plasmid, GE Healthcare). Bacteria were grown at 37 °C in LB medium complemented with 1% glucose, and protein expression was performed for 4 h after IPTG induction (final concentration of 0.2 mM) at 18 °C. Then, cells were harvested and resuspended in extraction buffer (PBS, 10% glycerol, 1% Triton X-100, 10 mM EDTA, and 2 mM DTT) complemented with a protease inhibitor cocktail (Complete, Roche). Cell lysates were obtained by incubation of 0.25 mg/mL lysozyme with the cell suspension in extraction buffer complemented with DNase followed by a brief sonication step. The soluble extract was isolated by centrifugation, and the GST fusion protein was purified on Glutathione Sepharose beads (GE Healthcare). After incubation of the soluble extracts for 3 h at 4 °C with resin beads (20 μL of resin beads/mL of soluble extract), unbound proteins were extensively washed away with a wash buffer (PBS, 10% glycerol, 1% Triton X-100, and 10 mM EDTA). The resin beads were then equilibrated in the acetylation reaction buffer [25 mM Hepes-KOH (pH 7.8), 1 mM tris(3-hydroxypropyl)phosphine, and 0.1 mM ETDA]. For acetylation reactions, resin beads carrying the CBP protein were used as a 50% slurry in the acetylation buffer. The amount of protein was estimated on a 10% polyacrylamide gel at a resin bead concentration of 2 mg/mL.

***In Vitro* Acetylation of Tau by CBP.** Tau proteins were dissolved at a concentration of 100 μM in acetylation reaction buffer complemented with 4 mM acetyl-coenzyme A (acetyl-CoA). After addition of 100 μL of CBP resin slurry/mL of acetylation reaction mixture, acetylation of Tau was performed at 25 °C for 16 h. The acetyltransferase activity was assessed on a peptide from the human thymine-DNA glycosylase under the same conditions.[25] In this substrate, the acetylation activity was assessed by MALDI-TOF MS (Ultraflex II, Bruker Daltonics) and the acetylation rate determined by reverse phase chromatography. As nonenzymatic acetylation reactions with acetyl-CoA were described in *in vitro* experiments,[26−28] we performed, as a control, acetylation reactions under the same conditions described above without CBP. An interaction mapping was performed with 100 μM [^{15}N]lysine selectively labeled Tau441 and 4 mM coenzyme A (CoA).

NMR Spectroscopy. For NMR experiments, Tau proteins were dissolved at concentrations of 0.3−0.4 mM in a buffer containing 50 mM Na_iPO_4 (pH 6.6), 25 mM NaCl, 2.5 mM EDTA, 2.5 mM dithiothreitol, and 10% D_2O. The proton frequencies were calibrated with 1 mM sodium 3-trimethylsilyl-3,3′,2,2′-d_4-propionate (TMSP) as a reference. ^{1}H−^{15}N HSQC spectra were recorded at 600 MHz on ^{15}N-labeled or ^{15}N- and ^{13}C-labeled proteins with 64 scans per increment, with 2048 and 256 points in the proton and nitrogen dimensions, respectively.

For the identification of the lysine acetylation state, ^{15}N HSQC-TOCSY spectra were recorded on [^{15}N]lysine selectively labeled Tau samples at 900 MHz and 293 K, with 32 scans per increment and a TOCSY mixing time of 120 ms. Spectral widths were 16.0, 9.0, and 11.0 ppm in ^{1}H (F3), ^{15}N (F2), and ^{1}H (F1) dimensions with 3072, 78, and 416 sample points, respectively, and centered on 4.7 and 123.5 ppm in the proton and nitrogen dimensions, respectively. For uniformly ^{15}N-labeled samples, spectra were acquired with a spectral width of 23 ppm centered on 118.5 ppm in the nitrogen dimension.

For lysine assignment in [^{15}N]lysine Tau samples, three-dimensional HN(CO)CACB experiments were performed with 32 scans per increment. Spectral widths were 14.0, 9.0, and 55.0 ppm in the ^{1}H, ^{15}N, and ^{13}C dimensions with 3072, 40, and 256 sample points and centered on 4.7, 123.5, and 43.5 ppm, respectively. For uniformly ^{15}N-labeled samples, HNCACB and HN(CA)NNH spectra were acquired with eight scans per increment. Spectral widths were 14.0 and 27 ppm in the proton (F3) and nitrogen (F2) dimensions centered on 4.7 and 118.5 ppm and sampled with 2048 and 80 points, respectively. For the third (F1) dimension that is either carbon or nitrogen, spectral widths were 57.0 and 22.9 ppm centered on 37.4 and 118.5 ppm, respectively, and sampled with 128 points.

For the calculation of overall acetylation levels, the backbone amide resonance of the K311 residue was used as a reference because it gives an isolated signal both in Tau441 and in Tau-F4 at 125.86 ppm (8.21 ppm in the ^{1}H dimension) in the ^{1}H−^{15}N HSQC spectrum and shows no shift at all after incubation with CBP. This resonance was arbitrarily used to define the integration value for a single amide proton, while the NHε-Ac indicator signal at 127.23 ppm (7.97 ppm in the ^{1}H dimension) corresponds to the sum of signals relative to every acetylated lysine residue. The overall acetylation level was then calculated by the relative integration of the NHε-Ac indicator signal on the K311 signal.

Acetylation levels at specific positions were measured in [^{15}N]lysine selectively labeled Tau samples by relative

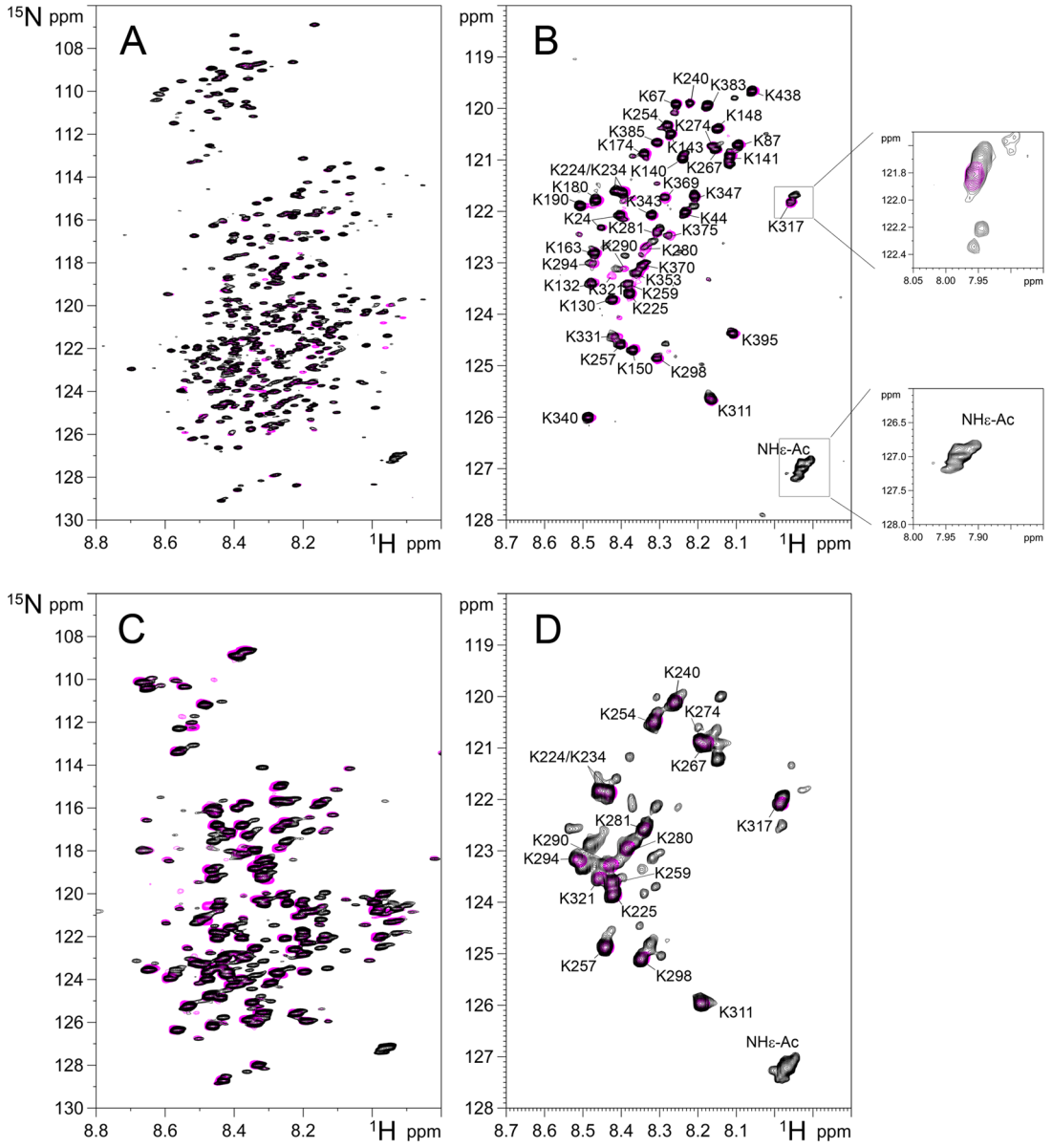

Figure 2. Detection of CBP-mediated acetylation in Tau proteins. Comparison of ^{1}H−^{15}N HSQC spectra of nonacetylated (pink) and CBP-acetylated (black) full-length Tau (A and B) or the Tau-F4 fragment (C and D). Proteins are either uniformly labeled with ^{15}N (A and C) or selectively labeled with [^{15}N]Lys (B and D). In panel B, indicator signals of acetylation (NHε-Ac, bottom boxed region) appear as several nonresolved resonances and indicate lysine Nε-acetylation at multiple sites. Spectral complexity generated by multiple proximal acetylations is illustrated by the resonance pattern of K317 (top boxed region). In the close-up of K317, the spectrum of the acetylated sample is depicted at lower levels for the detection of lower-intensity peaks.

integration of signals in the ^{1}H−^{15}N HSQC planes extracted from the ^{15}N HSQC-TOCSY experiments at 2.96 and 3.13 ppm in the proton dimension corresponding to nonacetylated and acetylated lysine residues, respectively. Acetylation rates were calculated for each lysine according to signal integration ratio of the resonance corresponding to the acetylated form(s) on the total integration corresponding to all forms. As a control, integrations in the two-dimensional (2D) ^{1}H−^{15}N HSQC experiment were calculated for residues exhibiting nonoverlapping signals in both their acetylated and non-acetylated states and give similar acetylation levels (Figure S1 of the Supporting Information). For overlapping resonances of K267 and K274 in its nonacetylated state, the assumption that integration values were equal for both residues was made. Acetylation levels of the nonenzymatic reaction with acetyl-CoA were calculated on the basis of signal integration in the 2D ^{1}H−^{15}N HSQC experiment. For overlapping resonances of K274^{Ac} and K141, an estimation of the acetylation level was made on the basis of the comparison of relative integrations of both K274 and K141 signals with those of the nonacetylated, control sample. The same strategy was employed for overlapping resonances of K174^{Ac} and K140. Similar levels of acetylation were detected for both lysine residues in (P)K224 and (P)K234 motifs, while unambiguous identification cannot be achieved. Similarly, one of the two (S)K pairs at positions 290 and 321 was found to be acetylated at a level of 5%.

Interactions between Tau and Heparin Monitored by NMR Spectroscopy. Heparin (heparin sodium salt from porcine intestinal mucosa; batch no. 031M1674 V) and thioflavin T (ThT) were purchased from Sigma. For interaction

dx.doi.org/10.1021/bi500006v | *Biochemistry* 2014, 53, 3020−3032

assays, selectively [^{15}N]Lys-labeled Tau441 in its nonacetylated and CBP-acetylated forms was dissolved at a concentration of 50 μM in 25 mM Na_iPO_4 (pH 6.6), 25 mM NaCl, 2.5 mM EDTA, 0.33 mM DTT (aggregation buffer), and 10% D_2O. Heparin was added at a final concentration of 12.5 μM, and ^{1}H−^{15}N HSQC spectra were recorded at 20 °C before and after overnight incubation at 37 °C. ^{1}H−^{15}N HSQC spectra were acquired with 2048 and 256 complex points in the proton and nitrogen dimensions, respectively, with 64 scans per increment. Spectral widths were 14.0 and 9 ppm centered on 4.7 and 123.5 ppm for the proton and nitrogen dimensions, respectively.

***In Vitro* Aggregation Kinetics Induced by Heparin.** For the aggregation assays, protein concentrations were normalized on the basis of their one-dimensional proton spectra acquired at 600 MHz. Tau proteins and heparin were mixed to a ratio of 4:1 as mentioned above in aggregation buffer with final Tau concentrations of 10 μM. Aggregation of Tau samples was performed without heparin as a control. ThT was extemporaneously prepared at a concentration of 5 mM and added to a final concentration of 50 μM before measurements. ThT emission was detected at 490 nm after excitation at 440 nm in 96-well plates on a PHERAStar (BMG LABTECH GmbH, Ortenberg, Germany). Five minute-step kinetics were performed for a total of 15 h for the nonacetylated, autoacetylated, and CBP-acetylated Tau441 as well as for the Tau-F4 fragment in its nonacetylated and CBP-acetylated state, with at least three independent experiments. Kinetic curves were fit to the following single-exponential association equation (eq 1).

$$Y = Y_{max}(1 - e^{-Kt}) \quad (1)$$

The supernatants of the aggregation mixtures of Tau441 or CBP-acetylated Tau441 were analyzed in sedimentation assays consisting of centrifugation at 100000*g* for 30 min at various aggregation times (0, 2, 4, and 16 h). Proteins in the supernatant were detected by Coomassie staining or Western blotting with Tau46 or anti-acetyllysine antibodies (Cell Signaling), respectively. After a 16 h incubation at 37 °C, aggregation mixtures were additionally analyzed by electron microscopy.

Electron Microscopy of Tau Fibrils. After aggregation, 10 μL of the fibrillization reaction mixture is applied to 400 mesh hexagonal Formvar-coated copper grids for 30 s. Excess liquid in the sample is drained on filter paper, washed twice with water, stained with 10 μL of 2% uranyl acetate for 60 s, and drained on filter paper. Samples were then analyzed using a Hitachi H7500 electron microscope operated at 80 kV.

RESULTS

Acetylation of Tau Protein Detected by NMR Spectroscopy. Full-length human Tau protein in its longest isoform (Tau441) was incubated with a fragment of mouse Creb-binding protein (CBP) (residues 1202−1849) that encompasses the acetyltransferase domain (CH2/HAT domain) as well as the CH3 protein-binding module. Acetylation reactions on uniformly ^{15}N-labeled or selectively [^{15}N]Lys-labeled, uniformly ^{13}C-labeled Tau441 proteins were conducted, and Tau acetylation was primarily assessed with the acquisition of standard ^{1}H−^{15}N HSQC NMR spectra. Novel amide resonances corresponding to the acetamide groups at the side chains of acetylated lysine residues (NHε-Ac) show up as indicator signals in an empty region of the spectrum (Figure 2).[22,23,29,30] Here, in the context of the full-length Tau protein, multiple nonresolved indicator signals were detected, suggesting that acetylation occurs at multiple sites (Figure 2). The relative integration of the NHε-Ac signals as compared to several isolated resonances among backbone amide functions gives an overall acetylation level of 6 ± 2 acetyl groups per molecule depending on the selected reference signal.

Variations of the chemical shift and signal intensity upon acetylation observed for backbone amide resonances in the ^{1}H−^{15}N HSQC spectrum cannot indicate the precise position of acetylation but rather regions that contain acetylation site(s) (Figure 2). As an example, a complex pattern of resonances was detected for K317 with at least four distinct signals. The shifted signal with a higher intensity comes from an acetylation event on a nearby residue, while acetylation on K317 was detected at a lower level (see Figure 4C,D), as will be detailed below. As previously shown,[6] the microtubule-binding repeats encompass most of the acetylated lysine residues while both the flanking proline-rich and the C-terminal domains contain few of them.

Contrary to phosphorylation that induces a downfield shift of Ser/Thr amide proton resonances within an empty area of the ^{1}H−^{15}N HSQC spectra of intrinsically disordered protein regions,[30] acetylation of lysine residues results in only small backbone amide chemical shift changes. Hence, the use of selective [^{15}N]lysine labeling facilitates the detection of resonance shifts in the ^{1}H−^{15}N HSQC spectra corresponding either to an acetylation site or to a nearby residue. However, this selective labeling prevents the full assignment through the HN(CA)NNH experiment. To overcome the assignment issue of redundant pairs (Table 1), the use of uniformly ^{15}N-labeled proteins provided the complete set of three-dimensional experiments for unambiguous assignments, however, at the expense of increasing spectral complexity. Therefore, we used the Tau-F4 protein, a shorter fragment encompassing residues 208−324,[31] to aid in the assignment of specific acetylation sites. We have produced the uniformly ^{15}N- and ^{13}C-labeled Tau-F4 protein in its wild-type or C291S mutant form (Tau-F4-C291S) to discriminate between both the SKCGS motifs around C291 and C322 residues.

Table 1. Summary of the Positions of Each (X)K Pair in Which X Is Any Amino Acid in Tau441

(X)K pair	position number of lysine residues[a]	(X)K pair	position number of lysine residues[a]
(P)K	180, 190, 224, 234	(Y)K	311, 395
(R)K	24	(W)K	–
(K)K	141, 225, 281, 370	(Q)K	163
(S)K	130, 132, 259, 290, 294, 317, 321, 353	(H)K	331, 375
(G)K	87, 148, 274	(I)K	298
(A)K	67, 143, 174, 240, 383, 385, 438	(L)K	44, 254, 267
(E)K	343	(D)K	140
(F)K	347	(M)K	–
(V)K	257, 340	(N)K	280, 369
(T)K	150	(C)K	–

[a]Numbering of the longest human Tau isoform (441 residues).

Assignment and Quantification of CBP Acetylation Sites in Tau Protein. In previous analyses of the effect of acetylation on chemical shifts in synthetic, homogeneously acetylated peptides, we found that the proton Hε resonance most sensitively reflects the acetylation state of lysine residues as compared to other proton or carbon resonances.[22] However,

dx.doi.org/10.1021/bi500006v | *Biochemistry* 2014, 53, 3020−3032

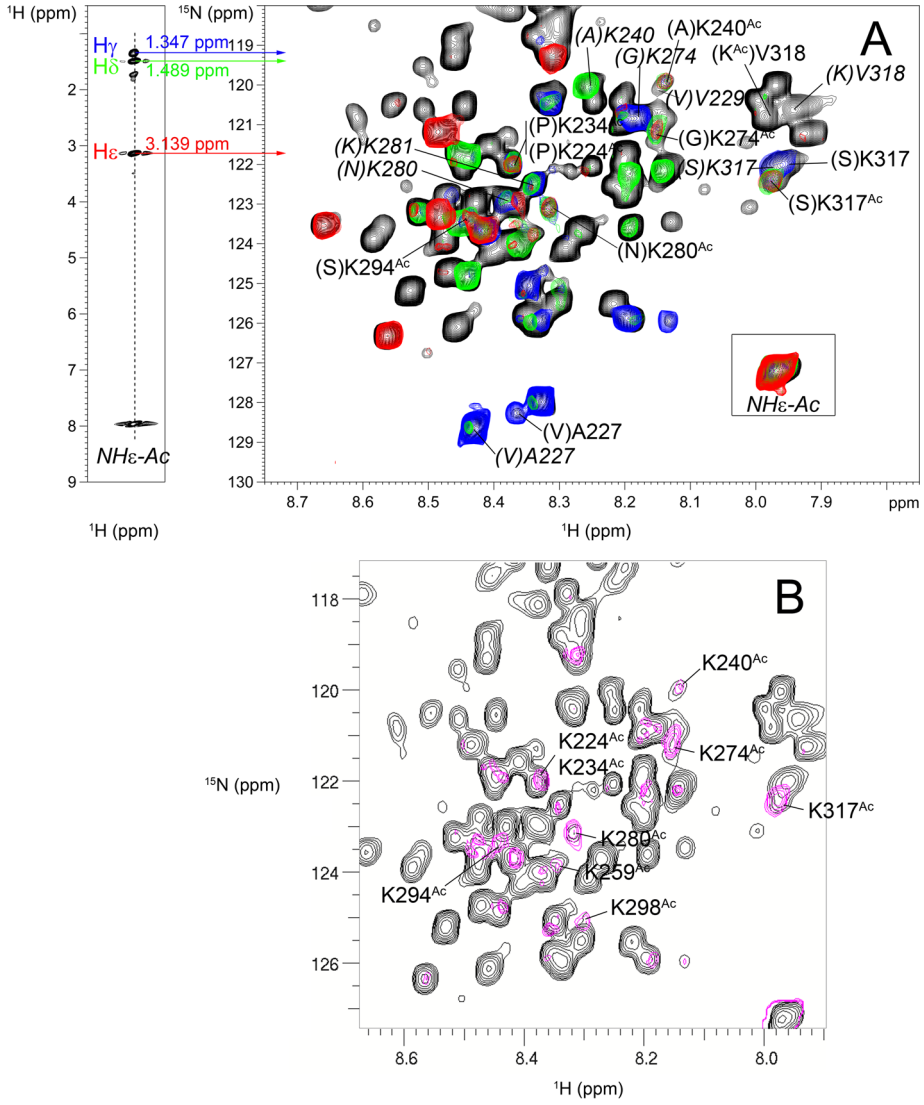

Figure 3. Detection and identification of acetylation sites in ^{13}C- and ^{15}N-labeled CBP-acetylated Tau-F4-C291S. (A) The left panel shows the $^{1}H-^{1}H$ plane of the TOCSY-HSQC experiment extracted at 127.23 ppm in the ^{15}N dimension showing the scalar couplings from the NHε-Ac amide proton of the acetylated lysine side chains at 7.97 ppm in the proton dimension. The Hγ (blue), Hδ (green), and Hε (red) proton chemical shifts of the acetylated lysine residues are given. The corresponding $^{1}H-^{15}N$ HSQC planes extracted from the TOCSY-HSQC experiment are represented in the right panel. The right panel shows a superimposition of the $^{1}H-^{15}N$ HSQC spectrum of the CBP-acetylated Tau-F4-C291S (black, A and B) and the $^{1}H-^{15}N$ planes of the TOCSY-HSQC spectrum extracted at 1.347 (blue), 1.489 (green), and 3.139 ppm (red) in the third dimension, corresponding to the Hγ, Hδ, and Hε resonances, respectively, of the acetylated lysine side chain. (B) Product plane (pink) obtained by the multiplication of the $^{1}H-^{15}N$ planes from the TOCSY-HSQC spectrum extracted at 1.347, 1.489, and 3.139 ppm described in panel A, highlighting the resonances corresponding to acetylation sites.

the Hε resonances of acetylated lysine residues are not significantly different from the Hδ resonances of arginine residues, necessitating a combination of the Hγ, Hδ, and Hε resonances for the detection and identification of acetylation sites (Figure 3A). For easier observation of acetylation sites, the product of $^{1}H-^{15}N$ planes extracted from the ^{15}N TOCSY-HSQC experiment at chemical shift values corresponding to Hγ, Hδ, and Hε resonances of acetylated lysines (Figure 3B) was calculated using a homemade algorithm for semiautomated protein assignment.[32] The Hγ, Hδ, and Hε chemical shift values of acetylated residues were determined in the 3D TOCSY-HSQC spectrum, using signal transfer originating from NHε-Ac, a signal specific to the acetylated residues (Figure 3A). No chemical shift variations were observed around 3.139, 1.489, and 1.347 ppm, corresponding to resonances of Hε, Hδ, and Hγ, respectively, as expected in the case of an IDP such as Tau protein, and as observed in peptide models.[22] These fixed values were thus used in the product plane approach. In accordance, small variations of ±0.01 ppm were found around the values of the side chain proton chemical shifts of acetylated lysines identified using this strategy (Figure S2 of the Supporting Information).

Homonuclear proton scalar correlations were used in the three-dimensional TOCSY-HSQC experiment to identify resonances corresponding to acetylated lysines in Tau samples after incubation with the acetyltransferase domain of CBP and acetyl-CoA. Hence, specific Hε resonances of either non-acetylated or acetylated lysine residues at 2.96 or 3.13 ppm, respectively, were determined within the $^{1}H-^{1}H$ plane extracted from the TOCSY-HSQC experiment recorded on

dx.doi.org/10.1021/bi500006v | Biochemistry 2014, 53, 3020−3032

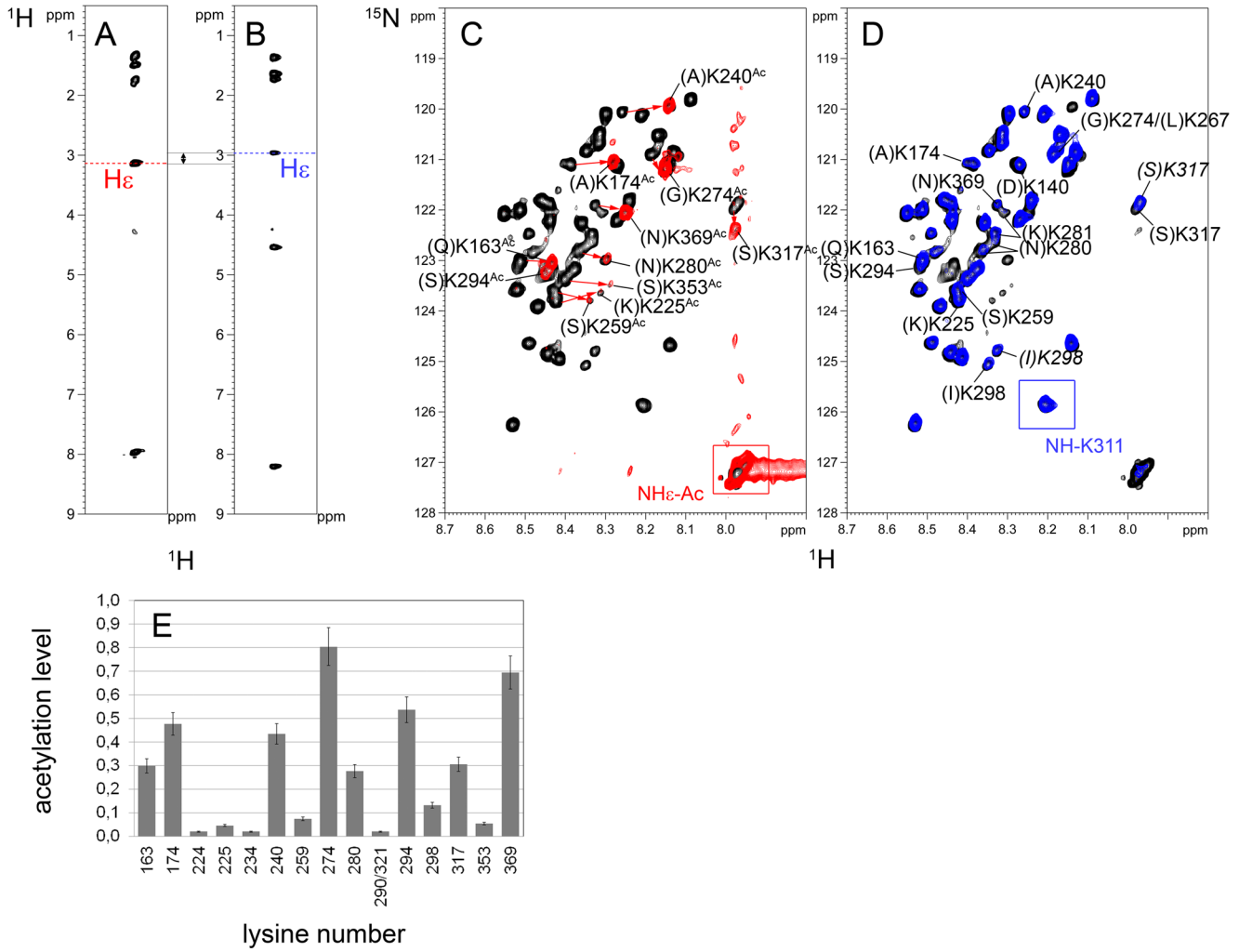

Figure 4. Strategy for identifying and quantifying lysine acetylation in full-length Tau. (A and B) $^{1}H-^{1}H$ TOCSY planes from the three-dimensional TOCSY-HSQC experiment corresponding to (A) the NHε-Ac signal (red boxed region in panel C) or (B) the backbone amide resonance of K311 (blue boxed region in panel D). (C and D) $^{1}H-^{15}N$ HSQC spectrum of the uniformly ^{13}C- and $[^{15}N]$Lys-labeled CBP-acetylated Tau441 (black spectra). $^{1}H-^{15}N$ HSQC planes from TOCSY-HSQC extracted at 3.13 ppm (C, red spectrum) and 2.96 ppm (D, blue spectrum) in the third dimension. Nonacetylated and acetylated lysine residues were assigned with the three-dimensional HN(CO)CACB experiment. Annotations with an Ac superscript correspond to resonances of the acetylated form of the corresponding residues. Italic annotations correspond to resonances of nonacetylated lysine residues that are not present in the nonacetylated control Tau spectrum. (E) Relative acetylation levels of the CBP-mediated acetylation. Only acetylated lysines are represented, and acetylation rates were calculated as described in Materials and Methods.

selectively $[^{15}N]$Lys-labeled Tau441 (Figure 4A–D). The backbone amide of the K311 residue that gives an isolated signal at 125.86 ppm (8.21 ppm in the ^{1}H dimension) in the $^{1}H-^{15}N$ HSQC spectrum and shows no shift at all after incubation with CBP was used to define the Hε resonance of the nonacetylated lysines, while the NHε-Ac indicator signal at 127.23 ppm (7.97 ppm in the ^{1}H dimension) was selected to define the Hε resonance of acetylated lysines. From these specific Hε resonances, we extract the $^{1}H-^{15}N$ planes corresponding to HSQC subspectra of lysine residues in both their nonacetylated and acetylated states, allowing for the discrimination between resonances of acetylated lysine from those of lysine residues that are close to an acetylation site (Figure 4C,D). Assignment of lysine residues was performed with the HN(CO)CACB experiment that provides an identification of the residue preceding each lysine (see Table 1).

In full-length Tau, this strategy allows for the detection of resonances corresponding to acetylated residues and the identification of acetylation sites (Figure 4A–D). The same strategy was applied in the Tau-F4 fragment (see Figure S3 of the Supporting Information) to discriminate between several lysine residues in identical pairs such as (A)K which is unique in Tau-F4 at position K240 and present at seven positions in full-length Tau. Similarly, the comparison of both acetylated Tau441 and Tau-F4 spectra allows discrimination between both (N)K pairs at positions 280 and 369. Furthermore, the distribution of acetylation can be detected at vicinal positions as exemplified with K298, for which a complex pattern of resonances is indicative of acetylation at both K298 and K294 (see Figure S3 of the Supporting Information). Although most of the acetylation sites of Tau441 are located within the Tau-F4 fragment, we identified three major acetylation sites specific for Tau441 as K163, K174, and K369. These three lysine residues were also identified as major acetylation sites by MS and mutational analyses in previous studies,[6,10] where it was shown that in-cell acetylation levels were strongly reduced in either the Tau-K163R/K174R/K180R mutant[6] or the Tau-

dx.doi.org/10.1021/bi500006v | Biochemistry 2014, 53, 3020–3032

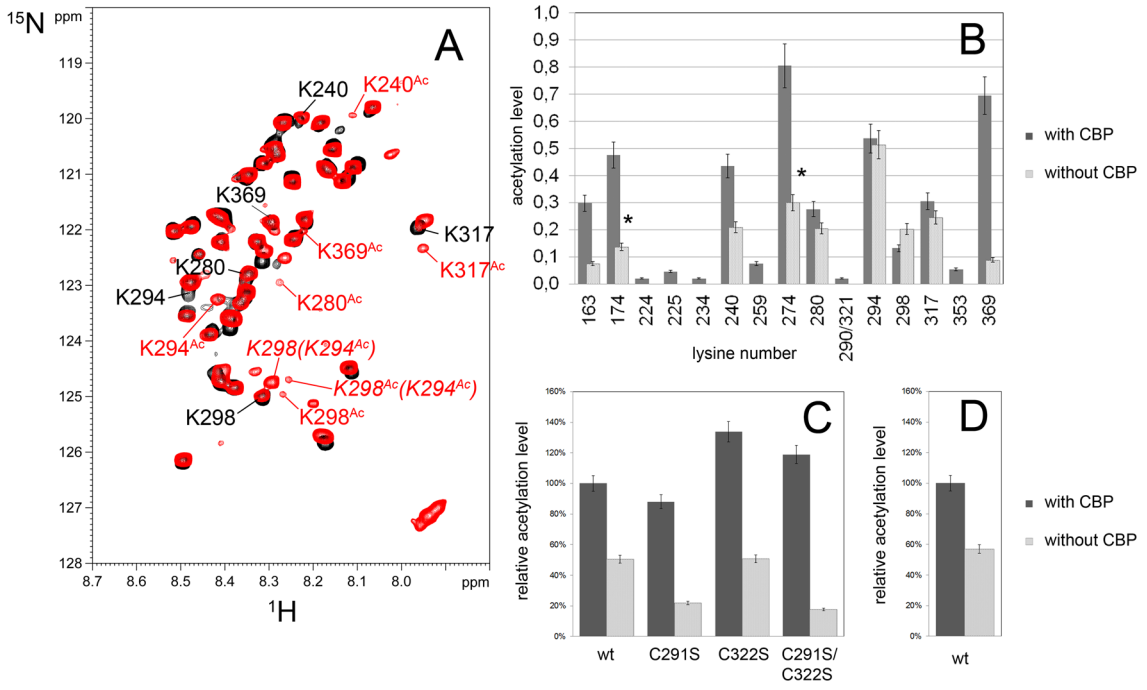

Figure 5. Nonenzymatic acetylation of Tau441. (A) $^{1}H-^{15}N$ HSQC spectrum of the autoacetylation reaction of wild-type Tau441 with acetyl-CoA (red) and control spectrum of Tau441 (black). (B) Quantification of the nonenzymatic reaction in Tau441. Acetylation rates of the nonenzymatic reaction with acetyl-CoA (light gray bars) are given for each lysine. CBP-mediated acetylation rates (dark gray bars) are added for comparison. Asterisks denote lysine residues for which the acetylation levels were estimated because of signal overlap of either the acetylated form (in the case of $K174^{Ac}$) or both the acetylated and nonacetylated form (in the case of K274). (C and D) Relative overall acetylation levels of Tau proteins acetylated in the presence (dark gray) or absence (light gray) of CBP in both wild-type Tau441 (D) and a series of Tau-F4 wild-type and mutant proteins (C). Overall acetylation levels were calculated by the relative integration of NHε-Ac on the K311 signal as described in Materials and Methods. The levels of 100% were arbitrarily assigned to the CBP-mediated acetylation of wild-type (wt) proteins.

K163R/K280R/K281R/K369R mutant.[10] These data indicate that *in vitro* acetylation with the recombinant CBP enzyme has a specificity similar to that observed in cellular models.

Interestingly, NMR detection of acetylation events at a per-residue resolution also provides a quantitative overview of CBP-mediated Tau acetylation and allows them to be sorted out. Major acetylation sites were found for lysines 163, 174, 240, 274, 280, 294, 298, 317, and 369. Other sites were acetylated at a lower level at positions 224, 225, 234, 259, 290/321, and 353 (Figure 4E). The relative acetylation levels were similar between Tau441 and Tau-F4 for the residues shared by both proteins.

Nonenzymatic Acetylation of Tau: Characterization of the Acetylation Pattern in the Absence of CBP and the Role of Cysteine Residues. An autoacetylation mechanism has been described for Tau, involving both cysteine residues at positions 291 and 322.[24] To evaluate its efficiency, we have compared the acetylation reactions with 4 mM acetyl-CoA in the presence and absence of CBP on wild-type Tau441 and Tau-F4 proteins, and in a series of Tau-F4 cysteine mutants (Tau-F4-C291S, Tau-F4-C322S, and Tau-F4-C291S/C322S) at a concentration of 100 μM (Figure 5). Because Tau-F4 and Tau441 contain 17 and 44 lysines, respectively, the molar ratio of acetyl-CoA to lysine is 2.35:1 for Tau-F4 and slightly less than 1:1 for full-length Tau.

We have detected for all proteins the indicator signal of lysine Nε-acetylation in the presence or absence of the acetyltransferase, confirming that acetylation of lysines occurs in the absence of CBP but, unexpectedly, also in the absence of any cysteine residues. These results suggest that Tau autoacetylation either requires residues other than cysteine and exploits a more complex pathway or is simply a chemical reaction between lysine and acetyl-CoA. In wild-type proteins, the nonenzymatic acetylation levels are significantly lower than the CBP-mediated acetylation level, although similar acetylation patterns are observed (Figure 5). The overall acetylation level upon nonenzymatic reaction was found to be half of the CBP acetylation rate as estimated from the integration of the indicator signals.

Mutation of both cysteine residues reduces the rate of the nonenzymatic reaction but does not prevent it. The individual mutation of each cysteine leads to opposite effects on the overall acetylation of Tau-F4. While C291 stimulates both the CBP-mediated and nonenzymatic acetylation with a more pronounced effect on the latter, C322 decreases the rate of the enzymatic reaction without a significant effect on the nonenzymatic one (Figure 5C).

Although we have detected lower overall levels of acetylation without acetyltransferase, the situation appears to be more complex when looking at the level of individual lysine residues. Typically, relatively high autoacetylation levels were found for lysines located in the MTBR and the immediate C-terminal extremity of the proline-rich domain, i.e., K240, K274, K280, K294, K298, and K317. Furthermore, autoacetylation of lysines close to cysteine residues in the primary sequence is strongly dependent on the latter: K294 and K298 autoacetylation is almost completely abolished by the C291 mutation, while that of K317 is affected by the C322 mutation (see Figure S4 of the Supporting Information). In the Tau-F4-2CS mutant lacking both cysteine residues, acetylation of the previously cited lysines is provided almost exclusively by CBP activities to a level comprised between one-third and half of the acetylation

dx.doi.org/10.1021/bi500006v | *Biochemistry* 2014, 53, 3020−3032

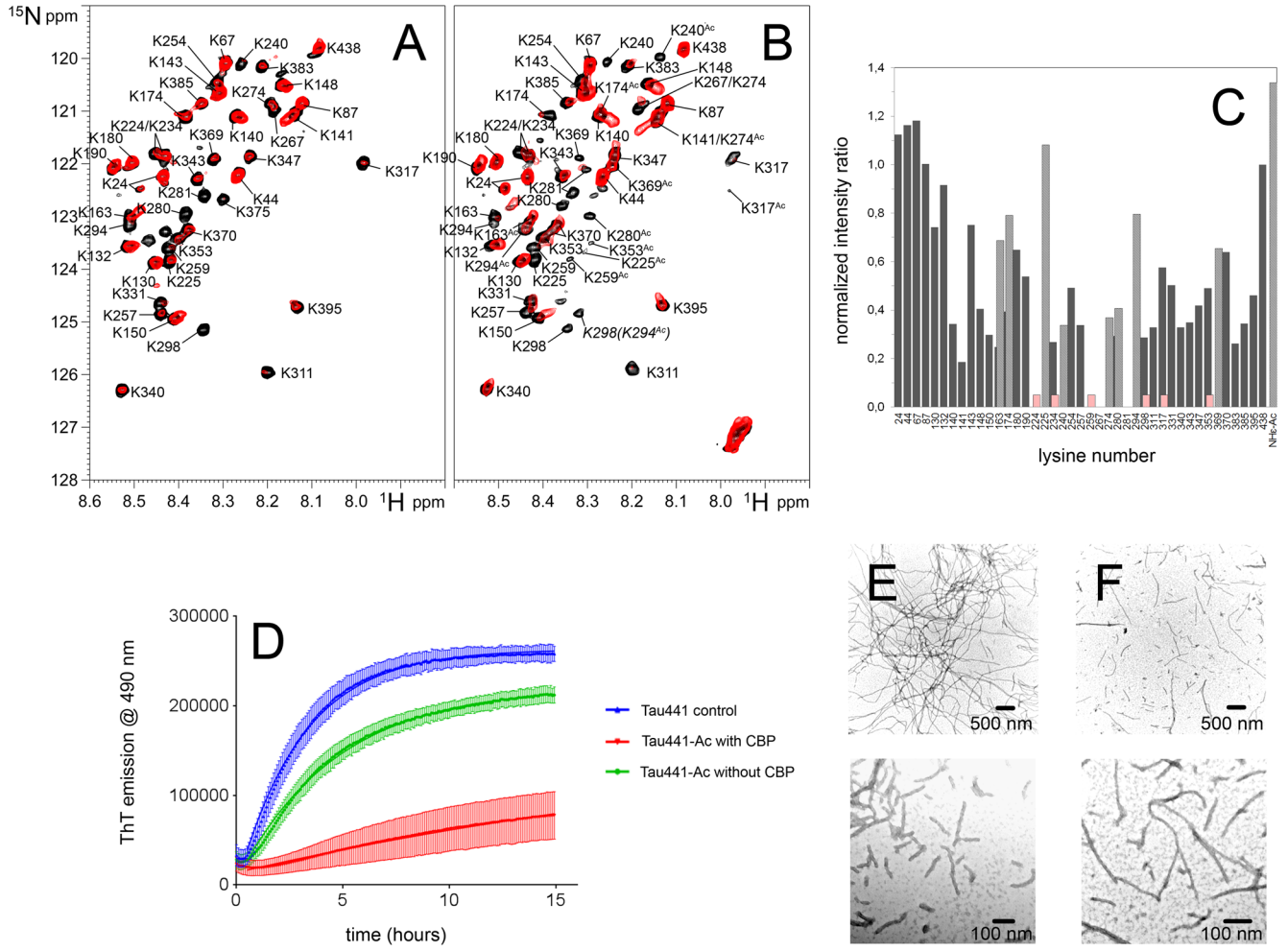

Figure 6. Interactions of CBP-acetylated Tau with heparin and effect of Tau acetylation on the kinetics of heparin-induced aggregation. (A and B) Interaction mapping of control Tau441 (A) and CBP-acetylated Tau441 (B) with heparin. Superimposition of ^{1}H−^{15}N HSQC spectra of Tau proteins at 50 μM without (black) and with (red) 12.5 μM heparin acquired at 293 K. (C) Mapping of heparin binding in CBP-acetylated Tau441. Variations of resonance intensities in the presence or absence of heparin normalized on the signal of K438. Resonances of nonacetylated and acetylated lysines are denoted with dark gray and light gray bars, respectively. Signals of acetylated lysines that are not detected upon additionof heparin because of the intensity beyond the detection limit are shown as red bars. (D) Kinetic curves of Tau aggregation monitored by thioflavin T fluorescence at 490 nm with Tau proteins at 10 and 2.5 μM heparin. The kinetic curve of the nonacetylated protein is colored blue, and those of the nonenzymatically and CBP-acetylated proteins are colored green and red, respectively. Each curve was obtained via at least three independent kinetic measurements. The aggregation profile of the CBP-acetylated Tau441 is measured on two different batches of acetylated proteins. (E and F) AD-like fibers induced by heparin in the NMR sample of Tau441 (E) and CBP-acetylated Tau441 (F) (as shown in panels A and B, respectively) after incubation for 16 h at 37 °C.

level measured in the wild-type protein (see Figure S4 of the Supporting Information). In contrast, for remote sites such as K163, K174, K240, K274, and K369, the difference between nonenzymatic and CBP-mediated acetylation is increased. For example, K240 in the proline-rich region is only weakly acetylated by nonenzymatic mechanisms and its acetylation is independent of both cysteine residues (see Figure S4 of the Supporting Information).

Acetylation Modulates Interactions with Heparin. Because polyanions such as heparin stimulate the formation of PHF-like fibers *in vitro* through interactions with lysine residues, we have evaluated the capacity of acetylated Tau to interact with heparin. We have monitored the interactions of native and CBP-acetylated Tau with heparin by NMR. Because the high molecular weight and size heterogeneity of heparin affect the resonance line shape of interacting residues and their neighbors in the primary sequence, we have mapped the modification of the signal intensity of lysine residues upon heparin addition in selectively [^{15}N]Lys-labeled Tau441 samples at a Tau:heparin molar ratio of 4:1 (Figure 6A−C). We have found a large binding interface encompassing half of the proline-rich domain (P2), as well as the whole MTBR and C-terminal regions in native Tau441 (see Figure S5 of the Supporting Information) as described previously.[33] This interface was not significantly changed in the CBP-acetylated Tau (Figure 6C). However, the signals of most of acetylated sites are relatively less reduced upon addition of heparin than their nonacetylated counterparts (see the resonances of K163, K174, K225, K240, K274, K280, K294, and K369 in their acetylated vs nonacetylated states). Importantly, we did not detect a significant decrease in signal intensity for the NHε-Ac resonances of the *N*-acetyllysines, indicating the absence of direct interactions between heparin and the acetylated side chains. The decrease in the resonance intensity observed for the backbone amide resonances of acetylated lysine residues could likely be assigned to the proximity of nonacetylated lysines that

dx.doi.org/10.1021/bi500006v | *Biochemistry* 2014, 53, 3020−3032

are still able to bind heparin, hence affecting the line shape of residues in their neighborhood. Because no interaction occurs with acetylation sites, it is likely that the binding interface with heparin is modified upon acetylation even though NMR did not allow a quantification of binding constants in this complex pattern of resonances and interactions.

CBP-Mediated Acetylation Slows the Kinetics of Fiber Formation. On the basis of these observations on heparin binding, we have investigated the role of acetylation in an *in vitro* aggregation assay in which Tau fibrillization was induced by heparin and aggregation kinetics were monitored by changes in thioflavin T (ThT) fluorescence. Given that lysine side chains are implicated in the dye-binding interface,[34] lysine acetylation could change the ThT binding capacity. Hence, we have monitored aggregation kinetics both by ThT fluorescence (Figure 6) and in a sedimentation assay (see Figure S6 of the Supporting Information). After overnight incubation at 37 °C, Tau:heparin mixtures (4:1 ratio) were analyzed by electron microscopy. Together, the data from these various experiments are in good agreement and show that acetylation of wild-type Tau441 significantly reduced the aggregation rate, indicating an inhibitory effect of acetylation on fiber formation while preserving the capacity to form PHF-like fibrils (Figure 6 and Figure S6 of the Supporting Information). Indeed, a significant increase in the magnitude of the ThT signal over time was detected with wild-type Tau441 together with a significant decrease in the protein concentration in the supernatant after ultracentrifugation of the aggregation reaction mixture. In contrast, CBP-acetylated Tau441 shows a smaller increase in ThT fluorescence, in agreement with no detectable change in the soluble protein concentration over incubation time as monitored in the sedimentation assay (see Figure S6 of the Supporting Information). Furthermore, acetylated proteins were detected using an anti-acetyllysine polyclonal antibody in the soluble and fibrillar fractions. To quantify the variation of aggregation kinetics upon acetylation, kinetic parameters were derived by fitting the experimental points to a single-exponential association curve (Table 2). We have found that

Table 2. Time Constants and Half-Times of the Aggregation Kinetic Curves for Tau Proteins Used in This Study Based on a Single-Phase Exponential Association Fit (eq 1)

	K (h^{-1})	$t_{1/2}$ (h)
Tau441	0.33 ± 0.01	2.11 ± 0.05
Tau441-Ac without CBP	0.21 ± 0.01	3.23 ± 0.09
Tau441-Ac with CBP	0.04 ± 0.02	19 ± 8

CBP acetylation strongly inhibits (almost 10-fold) the aggregation of Tau441. Furthermore, while acetylated Tau was still able to fibrillize, the amount of PHF-like fibrils and their average length were significantly reduced (Figure 6E,F). To evaluate the specific role of CBP acetylation, the aggregation kinetics of nonenzymatically acetylated Tau441 was monitored. As for CBP-acetylated Tau, a decrease in the aggregation kinetics was observed upon nonenzymatic acetylation, however to a lesser extent (Figure 6D and Table 2). Together, these data suggest that the aggregation rate is likely related to the acetylation level affecting, as a result, the binding to heparin.

DISCUSSION

Acetylation of the microtubule-associated Tau protein was recently found to be a pathological event in AD and other tauopathies[17,35] where it has been described as a posttranslational regulatory mechanism of Tau functions.[10,19] Furthermore, a deficit of proteasome-mediated degradation associated with an increased level of acetylation could be responsible for the accumulation of pathological phosphorylated Tau species leading to the formation of PHFs.[6] CBP and p300 acetylation sites were mapped by mass spectrometry after *in vitro* acetylation of Tau with recombinant acetyltransferases and tryptic digestion.[6,10] Although as many as 23 putatively acetyllysine residues were found, this methodology fails to give a quantitative view of the acetylation levels. Furthermore, the use of distinct acetyl specific antibodies targeting different Tau acetylation sites does not provide a global view of the multiple modifications among lysine residues dispersed along the Tau sequence. This analytical bias leads to significant discrepancies in the evaluation of the role of CBP/p300 acetylation in Tau functions. We previously used NMR for the characterization of Tau phosphorylation patterns by various kinases[36,37] and have also described its ability to analyze various posttranslational modifications in unfolded proteins[30] or in a globular domain.[38] Here, we use high-resolution NMR spectroscopy for the study of the acetylation pattern obtained via CBP acetyltransferase activity of the full-length Tau protein and in a shorter Tau-F4 fragment.

All the CBP acetylation sites were found in the central part of Tau, i.e., in the proline-rich domain and the microtubule-binding repeats. Among the highly acetylated sites were found lysine residues K163/K174 and K369 in the beginning of the proline-rich and C-terminal domains, respectively. The higher concentration of acetylation sites was localized in the repeat region, with K274 in R1, K280/K294 in R2, and K317 in R3, and in the flanking regions, with K240 and K369 (Figure 5). Minor sites with acetylation levels of <10% were found at K224, K225, K234, K259, K298, and K353. Our site identification is in good agreement with MS data that extensively described 23 acetylation sites obtained with *in vitro* acetylation by recombinant p300 and 87% sequence coverage.[6] However, two acetylation sites, K240 and K294, that were found to be heavily acetylated in our study have not been previously reported. Because of the distinct specificity of the close homologues p300 and CBP as shown for H3/H4 histone proteins,[27] it is likely that K240 and K294 were not acetylated by p300 and are therefore specific CBP acetylation sites.

Importantly, as previously described,[28,39] nonenzymatic acetylation occurs in the *in vitro* setup involving reaction with acetyl-CoA and cysteine residues. Such an acetyltransferase-independent acetylation has been described for Tau, implying both cysteine 291 and 322 in a mechanism of autoacetylation.[24] Hence, careful analysis must take into account these nonenzymatic processes as part of acetyltransferase activities upon investigation of acetylation patterns generated *in vitro*. We have detected the same overall pattern for nonenzymatic acetylation, however at levels lower than those obtained with the enzymatic reaction for most of the acetylation sites. The proficiency of the enzyme was then investigated for each individual site by comparison of the acetylation levels in the enzymatic and nonenzymatic reactions.

Even though cysteine residues play a role in the nonenzymatic acetylation by modulating the acetylation levels of

specific sites, the molecular mechanism remains unclear because lysine acetylation events were still detected in a Tau mutant lacking both cysteine residues. Acetylation of residues such as K294/K298 and K317 is mainly provided by the nonenzymatic reaction through residues C291 and C322, respectively (see Figure S4 of the Supporting Information). While C291 plays a positive role in Tau acetylation with CBP being present or not, C322 acts only by inhibiting CBP activity. Interestingly, the catalytic proficiency is at the lowest level for lysines located in repeats R2 and R3, i.e., from K280 to K317. In contrast, the proficiency of the enzyme is much higher for remote lysines such as K163, K174, K240, K274, and K369.

Interestingly, as the nonenzymatic and enzymatic reactions lead to nearly identical acetylation patterns, CBP is not essential for the substrate selectivity that is encoded in the Tau sequence itself and facilitates the acetyl transfer from the acetyl-CoA donor in only a site specific manner. Hence, lysine selectivity occurs in this intrinsically disordered protein even in the absence of an acetyltransferase, suggesting a crucial role of local charge distribution and/or accessibility due to long- and/or short-range intramolecular interactions. At the global level, Tau is a highly dynamic protein exhibiting an ensemble of overall extended conformations as primarily illustrated by the relatively poor dispersion of proton resonances in the NMR spectra. Nevertheless, Tau is not a fully statistical coil because it exhibits a transient global folding into a paperclip-like conformation where N- and C-termini establish transient contacts with the repeat domain.[40−43] This could hardly explain the limited accessibility for lysine acetylation in the same way that was used for any globular protein. Locally, a few short peptide stretches were shown to sample transient secondary structures.[42] Except for K274 and K280, which fall in the PHF6* sequence that has a propensity for β-structure, higher-level acetylation sites are not correlated with reported sequences of increased rigidity or exhibiting transient secondary structures. Remarkably, acetylation sites are missing from the entire acidic N-terminal domain (residues 1−150). Together, these data indicate that the selectivity of acetylation is mainly directed by the surrounding primary sequence of the lysine residues.

Interactions of acetylated Tau with heparin and its capacity for self-assembly involving heparin as an aggregation inducer have been examined. The ability of CBP-acetylated Tau to form insoluble PHF-like fibrils as monitored by thioflavin T fluorescence, a sedimentation assay, and electron microscopy was significantly weakened. We have found that acetylation of full-length Tau inhibits the formation of PHF-like fibrils by slowing the rate of aggregation but does not prevent it or perturb the nucleation step. Whereas CBP-mediated acetylation did not prevent interactions of Tau with heparin, acetylation sites are not directly involved in heparin binding (Figure 6C). Hence, it is likely that the Tau−heparin complexes involve lysine residues in their nonacetylated state. As the binding interface is large, implicating multiple low-affinity sites, lysine acetylation probably inhibits heparin binding by reducing the number of binding sites in a way that cannot be quantified by NMR given the complexity of both resonance and interaction patterns. Nonenzymatic reaction of Tau with acetyl-CoA reduces by 40% the aggregation rate. In contrast, CBP-mediated acetylation while accounting for twice the acetylation level of the nonenzymatic process leads to a 10-fold decrease in the aggregation rate without affecting the nucleation step. In accordance, we have found that CBP-acetylated Tau441 is still able to aggregate into PHF-like fibers in the presence of heparin, however to a lesser extent and by forming fibers with a shorter average length compared to those seen with non-acetylated Tau441. Interestingly, acetylated proteins were detected in the supernatant and pellet fractions of aggregation reaction mixtures, suggesting that acetylated Tau proteins are still able to fibrillize. Their aggregation propensity could be modulated by the acetylation level and/or acetylation state of some particular sites. Another possibility is that nonacetylated or weakly acetylated Tau proteins are involved in the nucleation step while proteins with higher levels of acetylation are further recruited in the elongation phase. However, given the heterogeneity of the acetylated Tau sample and the unknown pattern of interactions (epitopes and/or affinity) of the anti-acetyllysine antibody, we cannot reach a conclusion about the acetylation state of fibrillar proteins.

Recently, it has been shown that Tau acetylation was associated with pathological neurodegeneration in AD and other major tauopathies where acetylated K280 immunoreactivity colocalizes with several phospho- and conformation-dependent epitopes associated with moderate to late stages of AD. Acetylation was found at every pathological stage of AD and correlates specifically with insoluble Tau aggregates.[17] Hence, acetylation was proposed as a pathological mechanism that occurs sequentially in disease progression after early transformations such as hyperphosphorylation and misfolding, and before late events such as proteolysis and cell death.[17] However, the molecular mechanism by which acetylation exerts its pathological activity is not fully understood, and conflicting results still hamper the comprehension of the role of Tau acetylation in the aggregation process. Lysine residues were found in β-sheet structures of insoluble aggregates of various amyloidogenic proteins[44−46] as illustrated by the crystal structure of β-sheets consisting of short peptides from Tau PHF6 or Aβ in complex with orange G.[47] *In vitro*, lysine residues have been implicated in the binding of heparin,[33] and it was recently shown that the propagation of Tau pathology in AD, a process in which acetylation could be implicated,[18] was mediated by heparin sulfate proteoglycans on the cell surface.[48] On one hand, Tau acetylation was shown to promote aggregation in a K18 fragment and full-length Tau.[10] Such increased capacity to form pathological fibrils in an *in vitro* heparin-based assay could come from the neutralization of positively charged lysine residues upon acetylation, similar to the proposed mode of action of heparin. On the other hand, acetylation of the four KXGS motifs present in every repeat has been shown to decrease the extent of fibril assembly.[19] Despite the fact that they were all found to be acetylated at low levels by our NMR analysis, our data on Tau aggregation are in agreement with this inhibitory role of acetylation in PHF-like fibril formation that could be explained by weakened intermolecular interactions with the negatively charged heparin molecules. *In vivo*, however, lysine neutralization in conjunction with phosphorylation could be responsible of the stimulation of Tau fibrillization. Hence, the molecular mechanism of acetylation in Tau physiopathology, such as the effect of individual sites in the modulation of Tau functions, still needs to be investigated further for the perspective of therapeutic interference in the treatment of tauopathies.

■ ASSOCIATED CONTENT

Supporting Information

Comparison of acetylation levels calculated in $^{1}H-^{15}N$ planes extracted from the three-dimensional ^{15}N TOCSY-HSQC

experiment and the two-dimensional $^{1}H-^{15}N$ HSQC experiment, chemical shifts of side chain protons of acetylated lysines in [^{15}N-Lys/$^{13}C_u$]Tau441, assignment of acetylation sites in the Tau-F4 fragment, role of C291 and C322 residues of Tau in enzymatic and nonenzymatic lysine acetylation, NMR interaction mapping of Tau with heparin, and monitoring of aggregation reactions of nonacetylated and CBP-acetylated Tau441 by ThT fluorescence, a sedimentation assay, and electron microscopy. This material is available free of charge via the Internet at http://pubs.acs.org.

AUTHOR INFORMATION

Corresponding Author

*Unité de Glycobiologie Structurale et Fonctionnelle (CNRS UMR 8576), Université Lille-Nord de France, Cité Scientifique Bâtiment C9, 59655 Villeneuve d'Ascq Cedex, France. E-mail: caroline.smet@univ-lille1.fr. Fax: +33 (0)3 2043 6555. Phone: +33 (0)3 2043 4997.

Funding

This work was supported by the Laboratoire d'Excellence DISTALZ.

Notes

The authors declare no competing financial interest.

ACKNOWLEDGMENTS

The 600 and 900 MHz NMR facilities are funded by the European Community, the Centre National de la Recherche Scientifique (CNRS), the Région Nord-Pas de Calais (France), the University of Lille-Nord de France (Lille 1), and the Institut Pasteur de Lille.

ABBREVIATIONS

AD, Alzheimer's disease; CBP, cAMP-responsive element-binding protein (Creb)-binding protein; HSQC, heteronuclear single-quantum coherence; MTBR, microtubule-binding repeats; PHF, paired helical filaments; PTM, posttranslational modification; ThT, thioflavin T; TOCSY, total correlation spectroscopy; MALDI-TOF MS, matrix-assisted laser desorption ionization time-of-flight mass spectrometry.

REFERENCES

(1) Choudhary, C., Kumar, C., Gnad, F., Nielsen, M. L., Rehman, M., Walther, T. C., Olsen, J. V., and Mann, M. (2009) Lysine acetylation targets protein complexes and co-regulates major cellular functions. *Science 325*, 834−840.

(2) Ito, A., Kawaguchi, Y., Lai, C. H., Kovacs, J. J., Higashimoto, Y., Appella, E., and Yao, T. P. (2002) MDM2-HDAC1-mediated deacetylation of p53 is required for its degradation. *EMBO J. 21*, 6236−6245.

(3) Cripps, D., Thomas, S. N., Jeng, Y., Yang, F., Davies, P., and Yang, A. J. (2006) Alzheimer disease-specific conformation of hyperphosphorylated paired helical filament-Tau is polyubiquitinated through Lys-48, Lys-11, and Lys-6 ubiquitin conjugation. *J. Biol. Chem. 281*, 10825−10838.

(4) Tai, H. C., Serrano-Pozo, A., Hashimoto, T., Frosch, M. P., Spires-Jones, T. L., and Hyman, B. T. (2012) The synaptic accumulation of hyperphosphorylated tau oligomers in Alzheimer disease is associated with dysfunction of the ubiquitin-proteasome system. *Am. J. Pathol. 181*, 1426−1435.

(5) Mori, H., Kondo, J., and Ihara, Y. (1987) Ubiquitin is a component of paired helical filaments in Alzheimer's disease. *Science 235*, 1641−1644.

(6) Min, S. W., Cho, S. H., Zhou, Y., Schroeder, S., Haroutunian, V., Seeley, W. W., Huang, E. J., Shen, Y., Masliah, E., Mukherjee, C., Meyers, D., Cole, P. A., Ott, M., and Gan, L. (2010) Acetylation of tau inhibits its degradation and contributes to tauopathy. *Neuron 67*, 953−966.

(7) Petrucelli, L., Dickson, D., Kehoe, K., Taylor, J., Snyder, H., Grover, A., De Lucia, M., McGowan, E., Lewis, J., Prihar, G., Kim, J., Dillmann, W. H., Browne, S. E., Hall, A., Voellmy, R., Tsuboi, Y., Dawson, T. M., Wolozin, B., Hardy, J., and Hutton, M. (2004) CHIP and Hsp70 regulate tau ubiquitination, degradation and aggregation. *Hum. Mol. Genet. 13*, 703−714.

(8) Tan, J. M., Wong, E. S., Kirkpatrick, D. S., Pletnikova, O., Ko, H. S., Tay, S. P., Ho, M. W., Troncoso, J., Gygi, S. P., Lee, M. K., Dawson, V. L., Dawson, T. M., and Lim, K. L. (2008) Lysine 63-linked ubiquitination promotes the formation and autophagic clearance of protein inclusions associated with neurodegenerative diseases. *Hum. Mol. Genet. 17*, 431−439.

(9) Julien, C., Tremblay, C., Emond, V., Lebbadi, M., Salem, N., Jr., Bennett, D. A., and Calon, F. (2009) Sirtuin 1 reduction parallels the accumulation of tau in Alzheimer disease. *J. Neuropathol. Exp. Neurol. 68*, 48−58.

(10) Cohen, T. J., Guo, J. L., Hurtado, D. E., Kwong, L. K., Mills, I. P., Trojanowski, J. Q., and Lee, V. M. (2011) The acetylation of tau inhibits its function and promotes pathological tau aggregation. *Nat. Commun. 2*, 252.

(11) Goode, B. L., and Feinstein, S. C. (1994) Identification of a novel microtubule binding and assembly domain in the developmentally regulated inter-repeat region of tau. *J. Cell Biol. 124*, 769−782.

(12) Mukrasch, M. D., Biernat, J., von Bergen, M., Griesinger, C., Mandelkow, E., and Zweckstetter, M. (2005) Sites of tau important for aggregation populate β-structure and bind to microtubules and polyanions. *J. Biol. Chem. 280*, 24978−24986.

(13) Rizzu, P., Van Swieten, J. C., Joosse, M., Hasegawa, M., Stevens, M., Tibben, A., Niermeijer, M. F., Hillebrand, M., Ravid, R., Oostra, B. A., Goedert, M., van Duijn, C. M., and Heutink, P. (1999) High prevalence of mutations in the microtubule-associated protein tau in a population study of frontotemporal dementia in the Netherlands. *Am. J. Hum. Genet. 64*, 414−421.

(14) von Bergen, M., Barghorn, S., Li, L., Marx, A., Biernat, J., Mandelkow, E. M., and Mandelkow, E. (2001) Mutations of tau protein in frontotemporal dementia promote aggregation of paired helical filaments by enhancing local β-structure. *J. Biol. Chem. 276*, 48165−48174.

(15) Hurtado, D. E., Molina-Porcel, L., Iba, M., Aboagye, A. K., Paul, S. M., Trojanowski, J. Q., and Lee, V. M. (2010) Aβ accelerates the spatiotemporal progression of tau pathology and augments tau amyloidosis in an Alzheimer mouse model. *Am. J. Pathol. 177*, 1977−1988.

(16) Yoshiyama, Y., Higuchi, M., Zhang, B., Huang, S. M., Iwata, N., Saido, T. C., Maeda, J., Suhara, T., Trojanowski, J. Q., and Lee, V. M. (2007) Synapse loss and microglial activation precede tangles in a P301S tauopathy mouse model. *Neuron 53*, 337−351.

(17) Irwin, D. J., Cohen, T. J., Grossman, M., Arnold, S. E., Xie, S. X., Lee, V. M., and Trojanowski, J. Q. (2012) Acetylated tau, a novel pathological signature in Alzheimer's disease and other tauopathies. *Brain 135*, 807−818.

(18) Grinberg, L. T., Wang, X., Wang, C., Sohn, P. D., Theofilas, P., Sidhu, M., Arevalo, J. B., Heinsen, H., Huang, E. J., Rosen, H., Miller, B. L., Gan, L., and Seeley, W. W. (2013) Argyrophilic grain disease differs from other tauopathies by lacking tau acetylation. *Acta Neuropathol. 125*, 581−593.

(19) Cook, C., Carlomagno, Y., Gendron, T. F., Dunmore, J., Scheffel, K., Stetler, C., Davis, M., Dickson, D., Jarpe, M., Deture, M., and Petrucelli, L. (2014) Acetylation of the KXGS motifs in tau is a critical determinant in modulation of tau aggregation and clearance. *Hum. Mol. Genet. 23*, 104−116.

(20) Drewes, G., Trinczek, B., Illenberger, S., Biernat, J., Schmitt-Ulms, G., Meyer, H. E., Mandelkow, E. M., and Mandelkow, E. (1995) Microtubule-associated protein/microtubule affinity-regulating kinase (p110mark). A novel protein kinase that regulates tau-microtubule

interactions and dynamic instability by phosphorylation at the Alzheimer-specific site serine 262. *J. Biol. Chem. 270*, 7679−7688.
(21) Schneider, A., Biernat, J., von Bergen, M., Mandelkow, E., and Mandelkow, E. M. (1999) Phosphorylation that detaches tau protein from microtubules (Ser262, Ser214) also protects it against aggregation into Alzheimer paired helical filaments. *Biochemistry 38*, 3549−3558.
(22) Smet-Nocca, C., Wieruszeski, J. M., Melnyk, O., and Benecke, A. (2010) NMR-based detection of acetylation sites in peptides. *J. Pept. Sci. 16*, 414−423.
(23) Dose, A., Liokatis, S., Theillet, F. X., Selenko, P., and Schwarzer, D. (2011) NMR profiling of histone deacetylase and acetyl-transferase activities in real time. *ACS Chem. Biol. 6*, 419−424.
(24) Cohen, T. J., Friedmann, D., Hwang, A. W., Marmorstein, R., and Lee, V. M. (2013) The microtubule-associated tau protein has intrinsic acetyltransferase activity. *Nat. Struct. Mol. Biol. 20*, 756−762.
(25) Tini, M., Benecke, A., Um, S. J., Torchia, J., Evans, R. M., and Chambon, P. (2002) Association of CBP/p300 acetylase and thymine DNA glycosylase links DNA repair and transcription. *Mol. Cell 9*, 265−277.
(26) Kuo, Y. M., and Andrews, A. J. (2013) Quantitating the specificity and selectivity of Gcn5-mediated acetylation of histone H3. *PLoS One 8*, e54896.
(27) Henry, R. A., Kuo, Y. M., and Andrews, A. J. (2013) Differences in Specificity and Selectivity Between CBP and p300 Acetylation of Histone H3 and H3/H4. *Biochemistry 52*, 5746−5759.
(28) Dormeyer, W., Ott, M., and Schnolzer, M. (2005) Probing lysine acetylation in proteins: Strategies, limitations, and pitfalls of in vitro acetyltransferase assays. *Mol. Cell. Proteomics 4*, 1226−1239.
(29) Liokatis, S., Dose, A., Schwarzer, D., and Selenko, P. (2010) Simultaneous detection of protein phosphorylation and acetylation by high-resolution NMR spectroscopy. *J. Am. Chem. Soc. 132*, 14704−14705.
(30) Theillet, F. X., Smet-Nocca, C., Liokatis, S., Thongwichian, R., Kosten, J., Yoon, M. K., Kriwacki, R. W., Landrieu, I., Lippens, G., and Selenko, P. (2012) Cell signaling, post-translational protein modifications and NMR spectroscopy. *J. Biomol. NMR 54*, 217−236.
(31) Fauquant, C., Redeker, V., Landrieu, I., Wieruszeski, J. M., Verdegem, D., Laprevote, O., Lippens, G., Gigant, B., and Knossow, M. (2011) Systematic identification of tubulin-interacting fragments of the microtubule-associated protein Tau leads to a highly efficient promoter of microtubule assembly. *J. Biol. Chem. 286*, 33358−33368.
(32) Verdegem, D., Dijkstra, K., Hanoulle, X., and Lippens, G. (2008) Graphical interpretation of Boolean operators for protein NMR assignments. *J. Biomol. NMR 42*, 11−21.
(33) Sibille, N., Sillen, A., Leroy, A., Wieruszeski, J. M., Mulloy, B., Landrieu, I., and Lippens, G. (2006) Structural impact of heparin binding to full-length Tau as studied by NMR spectroscopy. *Biochemistry 45*, 12560−12572.
(34) Schutz, A. K., Soragni, A., Hornemann, S., Aguzzi, A., Ernst, M., Bockmann, A., and Meier, B. H. (2011) The amyloid-Congo red interface at atomic resolution. *Angew. Chem., Int. Ed. 50*, 5956−5960.
(35) Irwin, D. J., Cohen, T. J., Grossman, M., Arnold, S. E., McCarty-Wood, E., Van Deerlin, V. M., Lee, V. M., and Trojanowski, J. Q. (2013) Acetylated tau neuropathology in sporadic and hereditary tauopathies. *Am. J. Pathol. 183*, 344−351.
(36) Landrieu, I., Lacosse, L., Leroy, A., Wieruszeski, J. M., Trivelli, X., Sillen, A., Sibille, N., Schwalbe, H., Saxena, K., Langer, T., and Lippens, G. (2006) NMR analysis of a Tau phosphorylation pattern. *J. Am. Chem. Soc. 128*, 3575−3583.
(37) Landrieu, I., Leroy, A., Smet-Nocca, C., Huvent, I., Amniai, L., Hamdane, M., Sibille, N., Buee, L., Wieruszeski, J. M., and Lippens, G. (2010) NMR spectroscopy of the neuronal tau protein: Normal function and implication in Alzheimer's disease. *Biochem. Soc. Trans. 38*, 1006−1011.
(38) Smet-Nocca, C., Launay, H., Wieruszeski, J. M., Lippens, G., and Landrieu, I. (2013) Unraveling a phosphorylation event in a folded protein by NMR spectroscopy: Phosphorylation of the Pin1 WW domain by PKA. *J. Biomol. NMR 55*, 323−337.
(39) Dormeyer, W., Dorr, A., Ott, M., and Schnolzer, M. (2003) Acetylation of the HIV-1 Tat protein: An in vitro study. *Anal. Bioanal. Chem. 376*, 994−1005.
(40) von Bergen, M., Barghorn, S., Jeganathan, S., Mandelkow, E. M., and Mandelkow, E. (2006) Spectroscopic approaches to the conformation of tau protein in solution and in paired helical filaments. *Neurodegener. Dis. 3*, 197−206.
(41) Jeganathan, S., von Bergen, M., Brutlach, H., Steinhoff, H. J., and Mandelkow, E. (2006) Global hairpin folding of tau in solution. *Biochemistry 45*, 2283−2293.
(42) Mukrasch, M. D., Bibow, S., Korukottu, J., Jeganathan, S., Biernat, J., Griesinger, C., Mandelkow, E., and Zweckstetter, M. (2009) Structural polymorphism of 441-residue tau at single residue resolution. *PLoS Biol. 7*, e34.
(43) Schwalbe, M., Ozenne, V., Bibow, S., Jaremko, M., Jaremko, L., Gajda, M., Jensen, M. R., Biernat, J., Becker, S., Mandelkow, E., Zweckstetter, M., and Blackledge, M. (2014) Predictive atomic resolution descriptions of intrinsically disordered hTau40 and α-synuclein in solution from NMR and small angle scattering. *Structure 22*, 238−249.
(44) Sinha, S., Lopes, D. H., and Bitan, G. (2012) A Key Role for Lysine Residues in Amyloid β-Protein Folding, Assembly, and Toxicity. *ACS Chem. Neurosci. 3*, 473−481.
(45) Sinha, S., Lopes, D. H., Du, Z., Pang, E. S., Shanmugam, A., Lomakin, A., Talbiersky, P., Tennstaedt, A., McDaniel, K., Bakshi, R., Kuo, P. Y., Ehrmann, M., Benedek, G. B., Loo, J. A., Klarner, F. G., Schrader, T., Wang, C., and Bitan, G. (2011) Lysine-specific molecular tweezers are broad-spectrum inhibitors of assembly and toxicity of amyloid proteins. *J. Am. Chem. Soc. 133*, 16958−16969.
(46) Marshall, K. E., Morris, K. L., Charlton, D., O'Reilly, N., Lewis, L., Walden, H., and Serpell, L. C. (2011) Hydrophobic, aromatic, and electrostatic interactions play a central role in amyloid fibril formation and stability. *Biochemistry 50*, 2061−2071.
(47) Landau, M., Sawaya, M. R., Faull, K. F., Laganowsky, A., Jiang, L., Sievers, S. A., Liu, J., Barrio, J. R., and Eisenberg, D. (2011) Towards a pharmacophore for amyloid. *PLoS Biol. 9*, e1001080.
(48) Holmes, B. B., DeVos, S. L., Kfoury, N., Li, M., Jacks, R., Yanamandra, K., Ouidja, M. O., Brodsky, F. M., Marasa, J., Bagchi, D. P., Kotzbauer, P. T., Miller, T. M., Papy-Garcia, D., and Diamond, M. I. (2013) Heparan sulfate proteoglycans mediate internalization and propagation of specific proteopathic seeds. *Proc. Natl. Acad. Sci. U.S.A. 110*, E3138−E3147.
(49) Wolfe, M. S. (2009) Tau mutations in neurodegenerative diseases. *J. Biol. Chem. 284*, 6021−6025.